Drug Design, Development and Therapy

Dovepress
open access to scientific and medical research

Open Access Full Text Article

ORIGINAL RESEARCH

Synthesis and Biological Evaluations of Monocarbonyl Curcumin Inspired Pyrazole Analogues as Potential Anti-Colon Cancer Agent

This article was published in the following Dove Press journal:
Drug Design, Development and Therapy

Zhenli Min[1,2,*]
Yue Zhu[1,3,*]
Xing Hong[1]
Zhijun Yu[1,2]
Min Ye[1,2]
Qiong Yuan[1,2]
Xiamin Hu[4]

[1]Hubei Province Key Laboratory of Occupational Hazard Identification and Control, Wuhan University of Science and Technology, Wuhan 430081, People's Republic of China; [2]New Medicine Innovation and Development Institute, College of Medicine, Wuhan University of Science and Technology, Wuhan 430081, People's Republic of China; [3]Stem Cell Lab, Puren Hospital Affiliated to Wuhan University of Science and Technology, Wuhan, Hubei 430081, People's Republic of China; [4]College of Pharmacy, Shanghai University of Medicine & Health Sciences, Shanghai, People's Republic of China

*These authors contributed equally to this work

Purpose: The monocarbonyl analogs of curcumin (MCACs) have been widely studied for their promising antitumor activity. Pyrazole is a five-membered aromatic heterocyclic system with various bioactivities incorporated frequently in drugs. However, few of MCACs inspired pyrazole analogues were investigated. To search for more potent cytotoxic agents based on MCACs, a series of new 1,5-diaryl/heteroaryl-1,4-pentadien-3-ones inspired pyrazole moiety was synthesized and evaluated on their anti-colon cancer activities.

Methods: Fifteen new compounds were synthesized and characterized by spectral datum, and then they were tested preliminarily by MTT assay for their cytotoxic activities against a panel of four human cancer cell lines, namely, gastric (SGC-7901), liver (HepG2), lung (A549), and colon (SW620) cancer cells. Compound **7h** exhibited excellent selectivity and outstanding anti-proliferation activity against SW620 cells among these 15 compounds. Further, the mechanisms were investigated by transwell migration and invasion assay, clonogenic assay, cell apoptosis analysis, cell cycle analysis, Western blot analysis.

Results: The IC_{50} value of **7h** against SW620 cells was 12 nM, being more potent than curcumin (IC_{50} = 9.36 μM), adriamysin (IC_{50} = 3.28 μM) and oxaliplatin (IC_{50} = 13.33 μM). Further assays showed that **7h** inhibited SW620 cell migration, invasion and colony formation obviously, which was due to its ability to induce cell cycle arrest in the G2/M and S phases and apoptosis. Western blot assay revealed that **7h** decreased the protein expression of ATM gene, which may primarily contribute to its anticancer activity against SW620 cells.

Conclusion: A new MCACs **7h** was synthesized and found to exhibit excellent anti-proliferation activity against SW620 cells. Further studies indicated that **7h** exerted its anticancer activity against SW620 cells probably via decreasing the ATM protein expression. The present study suggested that **7h** was a promising candidate as an anti-colon cancer drug for future development.

Keywords: 1, 5-diheteroarylpenta-1, 4-dien-3-one, colon cancer, cell proliferation, cell apoptosis, ATM gene

Introduction

Colon cancer is the third most common cancer and the second leading cause of cancer death worldwide.[1] Although target therapies and immunotherapy have achieved progresses in recent years, their applications and efficacies are still far from satisfactory for an advanced-stage colon cancer.[2] Chemotherapy is still considered the most effective for colon cancer.[3] However, cytotoxic drugs, such as cisplatin and paclitaxel, can lead to side effects and chemoresistance, imposing

Correspondence: Xiamin Hu; Qiong Yuan
Tel +862165883592; +86 27 68893640
Email huxm@sumhs.edu.cn; yuanqiong@wust.edu.cn

submit your manuscript | www.dovepress.com
DovePress
http://doi.org/10.2147/DDDT.S244865

a financial burden on patients and impairing their quality of life. Therefore, development of a novel potent anti-colon cancer agent with a low toxicity is urgently required.

Natural products play an important role in a process of drug discovery, and many drugs used clinically are of natural origins. Curcumin is a primary bioactive compound isolated from the turmeric, a dietary spice made from the rhizome of *Curcuma longa* (Figure 1). It possesses versatile biological activities. However, curcumin has as yet achieved a limited success clinically although it had been studied in a number of clinical trials,[4] and even there have been some controversies about its potential as a pharmaceutical agent recently.[5–8] The nature of instability as well as pharmacokinetic deficiencies of curcumin resulted from an unstable β-diketone moiety are one of the reasons for the fails and controversies. In spite of these shortcomings, curcumin has still aroused interests of many scientists to overcome them as it is safe and a dietary spice in some countries. The problem can be addressed in part by a chemical structural modification of curcumin besides a pharmaceutical way.[9,10] Indeed, great attempts have already been made by researchers to chemical modifications, and a large number of curcumin analogues have been synthesized.[11–15] In this process, a major chemical class, namely the MCACs, evolves that is characterized by 1, 5-diaryl/heteroaryl penta-1, 4-dien-3-one and incorporating a range of alternative substituent groups into the terminal aryl rings. These MCACs display multiple biological activities, such as antitumor,[16–21] anti-inflammatory,[22–24] antioxidant[25] and neuroprotection.[25] Meanwhile, most of the MCACs show better stabilities and activities than curcumin does in both in vivo and in vitro model.

Among these derivatives, various aryl or heteroaryl rings were incorporated into the 1, 5-position of MCACs to explore bioactivities, including pyrazine,[17] chromone,[19] indole,[20] imidazole,[21,26] quinoline,[27] quinazoline,[28] and piperidone[29] moieties, nevertheless, few of which were related to pyrazolyl group. Pyrazole, as a five-membered aromatic heterocyclic system, has attracted considerable attentions in development of pharmacological molecules, and many marketed drugs (Figure 1) bearing this moiety display a variety of biological activities, such as anti-tumor (ruxolitinib, crizotinib), anti-inflammatory (Celecoxib), and antiobesity (Rimonabant).[30,31] Therefore, we envisioned that incorporating substituted pyrazole structure to replace the above-mentioned aryl or heteroaryl rings of MCACs may be beneficial to search for new anticancer drugs. In an effort to discover chemical entities active against colon cancer, this background motivated us to introduce pyrazole moiety to one terminal of MCACs and investigate their bioactivities (Figure 1). Presented here was a study on the synthesis and anti-cancer evaluations of a series of new MCACs which inspired a pyrazole moiety.

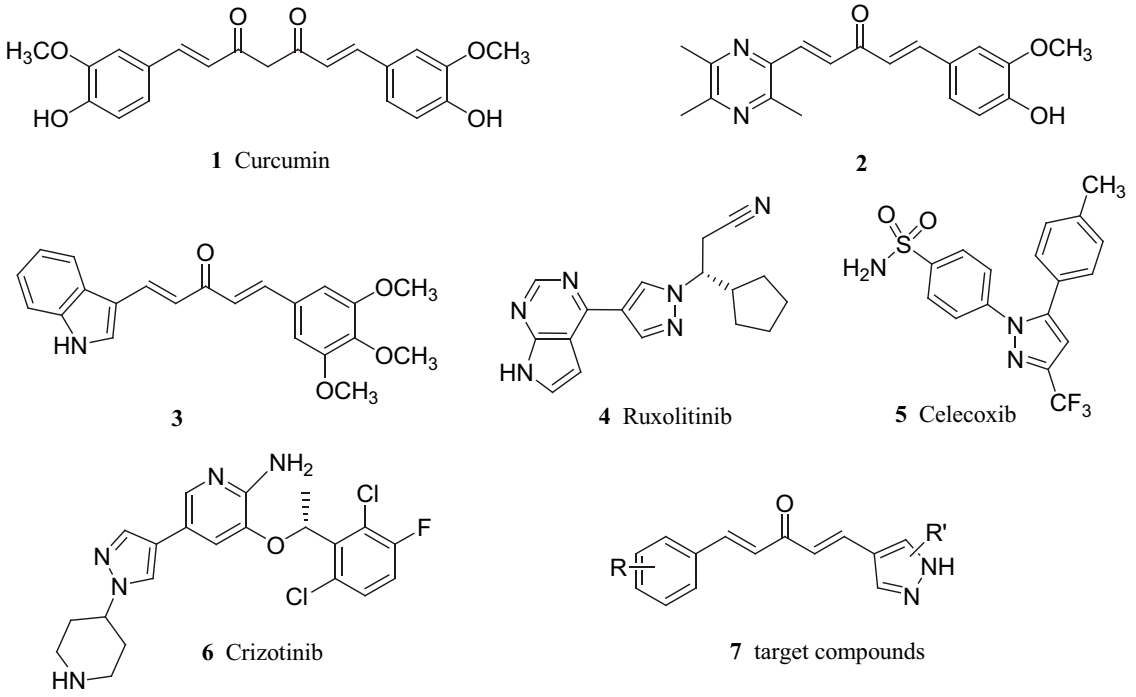

Figure 1 Chemical structures of Curcumin, MCACs, drugs and target compounds containing pyrazolyl ring.

Materials and Methods

Chemistry

All reagents and solvents were obtained from commercially available sources and were used without further purification. Reaction progress was monitored using analytical thin-layer chromatography (TLC) on precoated silica gel GF254 (Qingdao Haiyang Chemical Plant, Qing-Dao, China) plates and spots were detected under UV light (254 nm). Melting points were determined on a WRS-2B digital melting point apparatus and uncorrected. IR spectra were recorded using a Nicolet 380 Fourier-transform infrared (FTIR) spectrophotometer (Thermo, USA) from KBr pellets. ^{1}H NMR and ^{13}C NMR spectra were recorded on a Bruker AVANCE III-600 NMR spectrometer (Bruker Biospin Co., Switzerland) with tetramethylsilane (TMS) as the internal standard and $CDCl_3$ as solvent and known chemical shifts of residual proton signals of deuterated solvents (^{1}H NMR δ: 7.26 for $CDCl_3$ and δ: 3.33 for H_2O) or carbon signals of deuterated solvents (^{13}C NMR δ: 77.16 for $CDCl_3$) as internal standard. MS (ESI) measurement was conducted on an Agilent 1100 LC-MS spectrometer (Agilent, Palo Alto, USA).

The synthetic route of target molecules **7a**–**7o** was depicted in Scheme 1. All the target compounds and some intermediates were synthesized according to the following procedures.

Synthesis of 1-phenyl-3-methyl-5-pyrazolone 9[32]

Tungstophosphoric acid (1% mol) was dissolved in 40 mL water, and then phenylhydrazine (3 mmol) was added under stirring. To the mixture was slowly added ethyl acetoacetate (3 mmol) over a period of 20 min at room temperature. The mixture was further heated under reflux for 3 h. After completion of the reactions, the mixture was cooled to room temperature and solid was filtered off and washed with H_2O (40 mL). The crude products were dried and purified by recrystallization from ethanol to give **9** as a yellow powder, m.p: 125.5–127.1°C, yield: 78%.

Synthesis of 5-chloro-3-methyl-1-phenyl-1*H*-pyrazole-4-carbaldehyde 10

To a solution of 0.52 g compound**9** (3 mmol, 1.0 equiv) in dry DMF (2 mL) was added dropwise $POCl_3$ (0.42 mL, 4.5 mmol, 1.5 equiv) slowly while cooling in an ice-water bath. The mixture was stirred at 80°C for 2 h, and then cooled to room temperature, followed by pouring into ice-water (50 mL). The solution was neutralized by saturated $NaHCO_3$ solution and kept stirring for 30 min. The solid precipitated, filtered. The residue was recrystallized from ethanol to generate **10** as a light yellow solid, m.p: 145.0–146.5°C, yield: 38.2%.

General Procedure for Synthesis of 11a–11c

To a solution of 2-methoxyphenol, 3, 4-methylenedioxyphenol or ethanol (27 mmol, 1.0 equiv) in dry DMF (20 mL) was added KOH solid (1.73g, 29.7 mmol, 1.1 equiv) while stirring. The mixture was stirred at 40°C for 1 h, to which **10** (5.96g, 27 mmol, 1.0equiv) was added. The solution was stirred at 110°C for 5–6 h, and then cooled to ambient temperature, poured into ice-water. The mixture was stirred for 15 min, followed by extraction with ethyl acetate (3×20 mL). The combined organic layers were dried over Na_2SO_4 and concentrated and purified by silica gel column chromatography (hexanes/EtOAc = (10–6): 1) to give **11a**–**11c.**

5-(2-methoxyphenoxy)-3-methyl-1-phenyl-1H-pyrazole-4-carbaldehyde (11a)

A yellow solid, m.p: 73.4–74.5°C, 68.1% yield. ^{1}H NMR (600 MHz, $CDCl_3$) δ: 9.84 (s, 1H, CHO), δ 7.65 (d, J = 7.8 Hz, 2H,H-2′, 6′), 7.35 (t, J = 7.9 Hz, 2H, H-3′, 5′), 7.24 (t, J =7.4 Hz, 1H, H-4′), 7.10 (d, J = 8.3 Hz, 1H, H-6″), 7.05 (t, J = 7.4 Hz, 1H, H-4″), 7.02 (t, J = 7.8 Hz, 1H, H-5″), 6.95 (d, J = 8.2 Hz, 1H, H-3″), 3.83 (s, 3H, OCH_3), 2.53 (s, 3H, CH_3).

5-(benzo[d][1,3] dioxol-5-yloxy)-3-methyl-1-phenyl-1H-pyrazole-4-carbaldehyde (11b)

A white solid, m.p:106.6–107.4°C, 48.6% yield. ^{1}H-NMR (600 MHz, $CDCl_3$) δ: 9.58 (s, 1H, CHO), 7.63 (d, J = 7.7 Hz, 2H, H-2′, 6′), 7.43 (t, J = 7.9 Hz, 2H, H-3′, 5′), 7.34 (t, J = 7.4 Hz, 1H, H-4′), 6.69 (d, J = 8.5 Hz, 1H, H-5″), 6.59 (s, 1H, H-2″), 6.46 (d, J = 5.9 Hz, 1H, H-6″), 5.96 (s, 2H, OCH_2O), 2.53 (s, 3H, CH_3).

5-ethoxy-3-methyl-1-phenyl-1H-pyrazole -4-carbaldehyde (11c)

A light yellow oil, 40.1% yield. ^{1}H-NMR (600 MHz, $CDCl_3$) δ: 9.53 (s, 1H, CHO), 7.68 (d, J = 8.3 Hz, 2H, H-2′, 6′), 7.43 (t, J = 7.7 Hz, 2H, H-3′, 5′), 7.33 (t, J = 7.4 Hz, 1H, H-4′), 4.02 (q, J = 7.0 Hz, 2H, OCH_2), 2.53 (s, 3H, CH_3), 1.31 (t, J = 7.1 Hz, 3H, CH_3).

General Procedure for Synthesis of Various (*E*)-4-phenylbut-3-en-2-ones13a–13f

To a stirred solution of various benzaldehydes, **12** (3.6 mmol) in acetone (2 mL) was added 0.7 mL of 10%

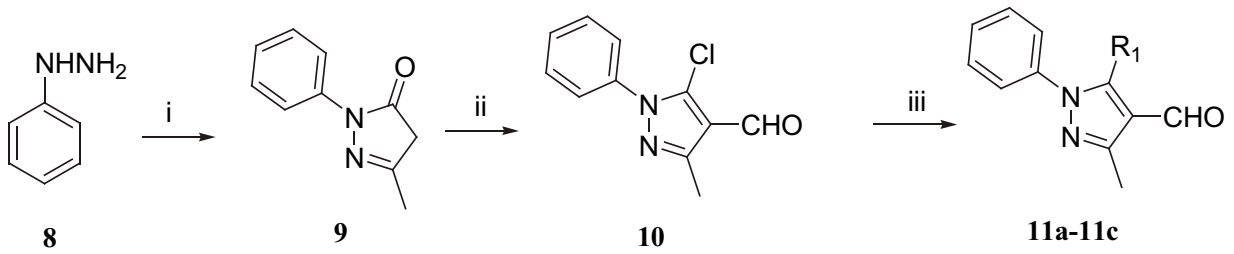

8 **9** **10** **11a-11c**

11a R_1=2-methoxyphenoxy,
11b R_1= C_2H_5O,
11c R_1=3,4-methylenedioxyphenoxy

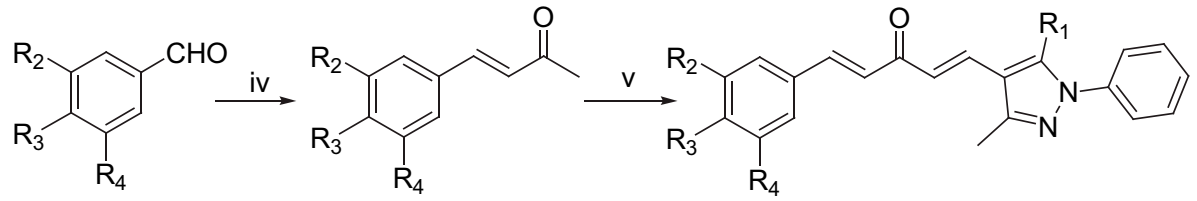

12 **13a-13f** **7a-7m**

13a R_2=H; R_3=H; R_4=H
13b R_2=OCH_3; R_3=OH; R_4=H
13c R_2=OCH_3; R_3=OCH_3; R_4=OCH_3
13d R_2=OCH_3; R_3=OCH_3; R_4=H
13e R_2=Br; R_3=OH; R_4=Br
13f R_2=Br; R_3=OH; R_4=Hr

13a-13f vi

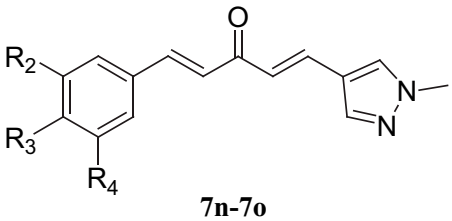

7n-7o

7a: R_1 =Cl ; R_2=H; R_3=H; R_4=H
7b: R_1 =Cl ; R_2=OCH_3; R_3=OH; R_4=H
7c: R_1 = Cl; R_2=OCH_3; R_3=OCH_3; R_4=OCH_3
7d: R_1 =Cl; R_2=H; R_3=OCH_3; R_4=H
7e: R_1 =Cl; R_2=Br; R_3=OH; R_4=Br
7f: R_1 =Cl; R_2=Br; R_3=OH; R_4=H
7m: R_1 =OC_2H_5; R_2=OCH_3; R_3=OH; R_4=H
7n: R_2=OCH_3; R_3=OCH_3; R_4=OCH_3
7o: R_2=OCH_3; R_3=OH; R_4=H

7g-7i: R_1=

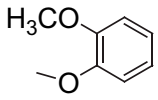

7g: R_2=OCH_3; R_3=OCH_3; R_4=H
7h: R_2=OCH_3; R_3=OCH_3; R_4=OCH_3
7i: R_2=OCH_3; R_3=OH; R_4=H

7j-7l: R_1=

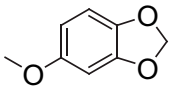

7j: R_2=OCH_3; R_3=OCH_3; R_4=H
7k: R_2=OCH_3; R_3=OCH_3; R_4=OCH_3
7l: R_2=OCH_3; R_3=OH; R_4=H

Scheme 1 Synthesis of target molecules 7a-7o; Reagents and conditions: (i) $CH_3COCH_2COOC_2H_5$, tungstophosphoric acid, H_2O, 100°C, 3h, 78%; (ii) $POCl_3$, DMF, 80°C, 3h, 42%; (iii) C_2H_5OH or substituted phenol, KOH, 100°C; (iv) CH_3COCH_3, 10%NaOH, rt, 2–4h, 47%; (v) 10 or 11a-11c, 10%NaOH, C_2H_5OH, rt, 12h, 20%; (vi) 1-methyl-1*H*-pyrazole-4-carbaldehyde, 10%NaOH, C_2H_5OH, rt, 12h, 17%.

aqueous NaOH solution at room temperature. The reaction was allowed to stir for 3–5 h till it was completed. The reaction mixture was poured into ice-water (30mL) and neutralized by 5% aqueous HCl while keeping stirring for 20 min. Then it was extracted with ethyl acetate (3×15 mL). The combined organic layers were dried over Na_2SO_4 and concentrated and purified by silica gel column chromatography (hexanes/EtOAc = (8–5): 1) to give **13a**–**13f.**

General Procedure for Synthesis of Target Compounds (7a–7o)

To a stirred solution of **13a–13f**(2.0 mmol) and **11a–11c** (2.2 mmol) in ethanol (10 mL) was added 0.9 mL of 10% aqueous NaOH solution at room temperature. The reaction was allowed to stir for 12–18 h till it was completed. The reaction mixture was poured into ice-water (50mL) and neutralized by 5% aqueous HCl while keeping stirring for

20 min. Then it was extracted with ethyl acetate (20×3 mL). The combined organic layers were dried over Na_2SO_4, concentrated and purified by silica gel column chromatography [hexanes/EtOAc = (7–3): 1] to give products, which were recrystallized from ethanol to afford **7a–7o.**

(1*E*, 4*E*)-1-(5-chloro-3-methyl-1-phenyl-1*H*-pyrazol-4-yl)-5-phenylpenta-1, 4-dien-3-one (7a)

A yellow solid, m.p:123.8–124.5°C, 16.1% yield. ^{1}H NMR (600 MHz, $CDCl_3$) δ: 7.74 (d, *J* = 15.9 Hz, 1H, vinyl H), 7.69 (d, *J* = 16.1 Hz, 1H, vinyl H), 7.63 (td, *J* = 5.4, 1.8 Hz, 2H, H-2′, 6′), 7.55 (dt, *J* = 7.3, 0.8 Hz, 2H, H-3′, 5′), 7.50 (td, *J* = 6.7, 1.6 Hz, 2H, H-2″, 6″), 7.45 (dt, *J* = 7.3, 1.3 Hz, 1H, H-4′), 7.43–7.41 (m, 3H, H-3″, 4″, 5″), 7.06 (d, *J* = 15.9 Hz, 1H, vinyl H), 7.05 (d, *J* = 16.1 Hz, 1H, vinyl H), 2.52 (s, 3H, CH_3). ^{13}C NMR (600 MHz, $CDCl_3$) δ: 188.62, 150.01, 143.09, 137.62, 134.81, 132.15, 130.44, 129.13, 128.92, 128.66, 128.38, 125.69, 124.98, 124.32, 114.14, 14.34. IR (KBr, cm^{-1}): 1651, 1621. ESI-MS m/z: 349.11$[M+H]^+$, calcd for $C_{21}H_{17}ClN_2O$: 348.10.

(1*E*, 4*E*)-1-(5-chloro-3-methyl-1-phenyl-1*H*-pyrazol-4-yl)-5-(3-methoxy-4-methylphenyl) penta-1, 4-dien-3-one (7b)

A yellow solid, m.p:144.9–146.1°C, 11.5% yield. ^{1}H NMR (600 MHz, $CDCl_3$) δ: 7.68 (d, *J* = 16.1 Hz, 1H, vinyl H), 7.67 (d, *J* = 15.8 Hz, 1H, vinyl H), 7.55 (d, *J* = 8.6 Hz, 2H, H-2′, 6′), 7.50 (t, *J* =7.8Hz, 2H, H-3′, 5′), 7.44 (t, *J*=7.4 Hz, 1H, H-4′), 7.19 (d, *J*= 8.2, 1.7Hz, 1H, H-6″), 7.12 (d, *J*= 1.7Hz, 1H, H-2″), 7.06 (d, *J* = 16.1 Hz, 1H, vinyl H), 6.95 (d, *J* = 8.2 Hz,1H, H-5″), 6.89 (d, *J* = 15.8 Hz, 1H, vinyl H), 5.97 (s, 1H, Ar-OH), 3.96 (s, 3H, OCH_3), 2.51 (s, 3H, CH_3). ^{13}C NMR (150 MHz, $CDCl_3$) δ: 188.53, 149.98, 148.30, 146.86, 143.43, 137.65, 131.71, 129.12, 128.63, 127.35, 124.98, 124.27, 123.73, 123.45, 114.87, 114.22, 109.83, 55.99, 14.30. IR (KBr, cm^{-1}): 3108, 1639. ESI-MS m/z: 395.12$[M+H]^+$, calcd for $C_{22}H_{19}ClN_2O_3$: 394.10.

(1*E*, 4*E*)-1-(5-chloro-3-methyl-1-phenyl-1*H*-pyrazol-4-yl)-5-(3, 4, 5-trimethoxyphenyl) penta-1, 4-dien-3-one (7c)

A yellow solid, m.p:87.5–88.7°C, 19.6% yield. ^{1}H-NMR (600 MHz, $CDCl_3$) δ: 7.69 (d, *J* = 16.1 Hz, 1H, vinyl H), 7.64 (d, *J* = 15.8 Hz, 1H, vinyl H), 7.54 (d, *J* = 7.7 Hz, 2H, H-2′, 6′), 7.49 (t, *J* = 7.8 Hz, 2H, H-3′, 5′), 7.43 (t, *J* = 7.3 Hz, 1H, H-4′), 7.06 (d, *J* = 16.1 Hz, 1H, vinyl H), 6.91 (d, *J* = 15.8 Hz, 1H, vinyl H), 6.84 (s, 2H, H-2″, 6″), 3.90 (s, 6H, OCH_3), 3.88 (s, 3H, OCH_3), 2.51 (s, 3H, CH_3). ^{13}C-NMR (150 MHz, $CDCl_3$) δ: 188.35, 153.44, 150.01, 143.16, 140.34, 137.61, 132.10, 130.27, 129.13, 128.66, 125.40, 124.96, 123.98, 114.17, 105.57, 60.98, 56.19, 14.33. ESI-MS m/z: 439.14$[M+H]^+$, calcd for $C_{24}H_{23}ClN_2O_4$: 438.13.

(1*E*, 4*E*)-1-(5-chloro-3-methyl-1-phenyl-1*H*-pyrazol-4-yl)-5-(3, 4-dimethoxyphenyl) penta-1, 4-dien-3-one (7d)

A yellow solid, m.p: 137.9–139.8°C, 50.1% yield.^{1}H-NMR (600 MHz, $CDCl_3$) δ: 7.68 (d, *J* = 16.0 Hz, 2H, vinyl H), 7.54 (d, *J* = 7.5 Hz, 2H, H-2′, 6′), 7.49 (t, *J* = 7.8 Hz, 2H, H-3′, 5′), 7.43 (t, *J* = 7.3 Hz, 1H, H-4′), 7.20 (dd, *J* = 8.2, 1.6 Hz, 1H, H-6″), 7.14 (d, *J* = 1.4 Hz, 1H, H-2″), 7.05 (d, *J* = 16.1 Hz, 1H, vinyl H), 6.90 (d, *J* = 15.9 Hz, 1H, vinyl H), 6.88 (d, *J* = 8.3 Hz, 1H, H-5″), 3.94 (s, 3H, OCH_3), 3.92 (s, 3H, OCH_3), 2.51 (s, 3H, CH_3). ^{13}C NMR (150 MHz, $CDCl_3$) δ: 188.45, 151.35, 149.97, 149.22, 143.19, 137.64, 131.73, 129.12, 128.62, 127.76, 124.96, 124.22, 124.02, 123.16, 114.21, 111.06, 109.87, 55.98, 55.93, 14.33. IR (KBr, cm^{-1}): 1657.6, 1591.1. ESI-MS m/z: 409.13$[M+H]^+$, calcd for $C_{23}H_{21}ClN_2O_3$: 408.12.

(1*E*, 4*E*)-1-(5-chloro-3-methyl-1-phenyl-1*H*-pyrazol-4-yl)-5-(3,5-dibromo-4-hydroxyphenyl)penta-1,4-dien-3-one (7e)

A yellow solid, m.p: 198.2–200.9°C, 56.5% yield. ^{1}H-NMR (600 MHz, $CDCl_3$) δ: 7.72 (s, 2H, H-2″, 6″), 7.69 (d, *J* = 16.1 Hz, 1H, vinyl H), 7.55–7.52 (m, 3H, vinyl H, H-2′, 6′), 7.51–7.48 (m, 2H, H-3′, 5′), 7.44 (tt, *J* = 7.3, 1.3 Hz, 1H, H-4′), 6.99 (d, *J* = 16.1 Hz, 1H, vinyl H), 6.91 (d, *J* = 15.8 Hz, 1H, vinyl H), 6.15 (s, 1H,Ar-OH), 2.50 (s, 3H, CH_3). ^{13}C-NMR (150 MHz, $CDCl_3$) δ: 187.86, 150.92, 150.09, 139.69, 137.57, 132.57, 131.85, 130.01, 129.15, 128.82, 128.71, 125.74, 124.98, 124.17, 114.07, 110.45, 14.33. IR (KBr, cm^{-1}): 3068, 1643, 1574. ESI-MS m/z: 534.94$[M+H]^+$, calcd for $C_{22}H_{17}Br_2ClN_2O_2$: 534.93.

(1*E*, 4*E*)-1-(5-chloro-3-methyl-1-phenyl-1*H*-Pyrazol-4-yl)-5-(3-bromo-4-hydroxyphenyl) penta-1, 4-dien-3-one (7f)

A yellow solid, m.p:187.2–188.4°C, 50.5%yield. ^{1}H NMR (600 MHz, $CDCl_3$) δ: 7.75 (d, *J* = 1.9 Hz, 1H, H-1″), 7.68 (d, *J* = 16.1 Hz, 1H, vinyl H), 7.61 (d, *J* = 15.8 Hz, 1H, vinyl H), 7.55 (d, *J* = 7.9 Hz, 2H, H-2′, 6′), 7.50 (td, *J* = 8.2, 1.9 Hz, 2H, H-3′, 5′), 7.49 (d, *J* = 1.8 Hz, 1H, H-6″), 7.43 (t, *J* = 7.3 Hz, 1H, H-4′), 7.05 (d, *J* = 8.4 Hz, 1H, H-5″), 7.01 (d, *J* = 16.1 Hz, 1H, vinyl H), 6.91 (d, *J* = 15.8 Hz, 1H, vinyl H), 5.85 (s, 1H, Ar-OH), 2.50 (s, 3H, CH_3).^{13}C NMR (150 MHz, $CDCl_3$) δ: 188.30, 154.22, 150.03, 141.30, 137.60, 132.20, 132.07, 129.56, 129.13, 129.07, 128.71, 128.68, 124.99, 124.63,

124.54, 124.34, 116.53, 114.17, 114.13, 110.88, 14.33. IR (KBr, cm^{-1}): 3066, 1616, 1596. ESI-MS m/z: 443.01[M +H]$^+$, calcd for $C_{21}H_{16}BrClN_2O_2$: 442.99.

(1*E*, 4*E*)-1-(5-(2-methoxyphenoxy)-3-methyl-1-phenyl-1*H*-pyrazol-4-yl)-5-(3, 4-dimethoxyphenyl) penta-1,4-dien-3-one (7g)

A yellow solid, m.p:159.7–160.2°C, 10.5% yield.^{1}H NMR (600 MHz, $CDCl_3$) δ: 7.65 (d, *J* = 7.8 Hz, 2H, H-2′, 6′), 7.47 (d, *J* = 16.0 Hz, 1H, vinyl H), 7.44 (d,*J* = 15.9 Hz, 1H, vinyl H), 7.35 (t, *J* = 7.9 Hz, 2H, H-3′, 5′), 7.24 (t, *J* =7.4 Hz, 1H, H-4′),7.10 (dd, *J* =8.3, 1.9 Hz, 1H, H-4‴), 7.04 (d, *J* = 1.7 Hz, 1H, H-6″), 7.02 (td, *J* = 8.4, 1.3 Hz, 1H, H-5‴), 6.95 (dd, *J* = 8.2, 1.2 Hz, 1H, H-6‴), 6.86 (d, *J* = 8.3 Hz, 1H, H-2″), 6.78 (dd, *J* = 8.3, 1.3 Hz, 1H, H-5″), 6.75 (d, *J* = 15.9 Hz, 1H, vinyl H), 6.70–6.68 (m, 2H, H-3‴, vinyl H), 3.91 (s, 6H, OCH_3), 3.90 (s, 3H, OCH_3),2.49 (s, 3H, CH_3). ^{13}C NMR (150 MHz, $CDCl_3$) δ: 188.74, 151.18, 149.55, 149.20, 148.97, 148.29, 144.84, 142.48, 137.48, 131.34, 129.00, 127.92, 127.30, 124.69, 124.47, 123.29, 122.80, 122.35, 121.11, 115.83, 112.94, 111.06, 109.86, 105.40, 56.20, 55.96, 55.91, 14.30. IR (KBr, cm^{-1}): 1621, 1591. ESI-MS m/z: 497.20 [M+H]$^+$, calcd for $C_{30}H_{28}N_2O_5$: 496.20.

(1*E*, 4*E*)-1-(5-(2-methoxyphenoxy)-3-methyl-1-phenyl-1*H*-pyrazol-4-yl)-5-(3,4,5-trimethoxyphenyl)penta-1,4-dien-3-one (7h)

A yellow solid, m.p:144.2–144.3°C, 10.9% yield.^{1}H-NMR (600 MHz, $CDCl_3$) δ: 7.65 (d, *J* = 7.7 Hz, 2H, H-2′, 6′), 7.48 (d, *J* = 15.9 Hz, 1H, vinyl H), 7.40 (d, *J* = 15.9 Hz, 1H, vinyl H), 7.35 (t, *J* = 7.9 Hz, 2H, H-3′, 5′), 7.25 (t, *J* =4.3 Hz, 1H, H-4′), 7.02 (td, *J* = 8.3, 1.4 Hz, 1H, H-4‴), 6.94 (dd, *J* = 8.2, 1.2 Hz, 1H, H-6‴), 6.78 (dd, *J* = 8.5, 1.4 Hz, 1H, H-5‴),6.76 (d, *J* = 15.9 Hz, 1H, vinyl H), 6.75 (s, 2H, H-2″, 6″), 6.72 (d, *J* = 15.9 Hz, 1H, vinyl H), 6.68 (dd, *J* = 8.1, 1.4 Hz, 1H, H-3‴), 3.90 (s, 3H, OCH_3), 3.89 (s, 6H, OCH_3),3.87 (s, 3H, OCH_3), 2.49 (s, 3H, CH_3). ^{13}C-NMR (150 MHz, $CDCl_3$) δ: 188.63, 153.40, 149.58, 148.93, 148.32, 144.83, 142.47, 140.17, 137.43, 131.69, 130.43, 129.01, 127.36, 125.85, 124.67, 123.06, 122.37, 121.12, 115.78, 112.91, 105.46, 105.41, 60.98, 56.20, 56.17, 14.31. IR (KBr, cm^{-1}): 1667, 1619. ESI-MS m/z: 527.22 [M+H]$^+$, calcd for $C_{31}H_{30}N_2O_6$: 526.21.

(1*E*, 4*E*)-1-(5-(2-methoxyphenoxy)-3-methyl-1-phenyl-1*H*-pyrazol-4-yl)-5-(4-hydroxy-3-methoxyphenyl)-penta-1,4-dien-3-one (7i)

A yellow solid, m.p:116.4–118.1°C, 11.4% yield. ^{1}H-NMR (600 MHz, $CDCl_3$) δ: 7.66 (d, *J* = 7.7 Hz, 2H, H-2′, 6′), 7.46 (d, *J* = 16.0 Hz, 1H, vinyl H), 7.42 (d, *J* = 15.9 Hz, 1H, vinyl H), 7.35 (t, *J* = 7.9 Hz, 2H, H-3′, 5′), 7.25 (d, *J* = 5.6 Hz, 1H, H-4′), 7.06 (d, *J* = 8.2 Hz, 1H, H-4‴), 7.03 (t, *J* = 6.6 Hz, 2H, H-5‴, 6‴), 6.96 (d, *J* = 7.9Hz, 1H, H-6″), 6.91 (d, *J* = 8.2 Hz, 1H, H-6″), 6.78 (t, *J* = 8.0 Hz, 2H, H-3‴), 6.74 (d, *J* = 16.0 Hz, 1H, vinyl H), 6.70 (s, 1H, H-2″), 6.67 (d, *J* = 15.9 Hz, 1H, vinyl H), 5.91 (s, 1H, Ar-OH), 3.92 (s, 3H, OCH_3), 3.90 (s, 3H, OCH_3), 2.49 (s, 3H, CH_3).^{13}C NMR (150 MHz, $CDCl_3$) δ: 188.81, 149.55, 148.98, 148.31, 148.04, 146.78, 144.84, 142.69, 137.47, 131.34, 129.00, 127.51, 127.31, 124.70, 124.16, 123.29, 123.10, 122.38, 121.11, 115.84, 114.75,112.97, 109.68, 105.38, 56.21, 55.94, 14.28. IR (KBr, cm^{-1}): 3435, 1642, 1564. ESI-MS m/z: 483.17 [M +H]$^+$, calcd for $C_{29}H_{26}N_2O_5$: 482.16.

(1*E*, 4*E*)-1-(5-(benzo[d][1,3]dioxol-6-yloxy)-3-methyl-1-phenyl-1*H*-pyrazol-4-yl)-5-(3,4-dimethoxyphenyl)penta-1,4-dien-3-one (7j)

A yellow solid, m.p:151.4–153.6°C, 12.8% yield. ^{1}H-NMR (600 MHz, $CDCl_3$) δ: 7.60 (dd, *J* = 8.6, 1.1 Hz, 2H, H-2′, 6′), 7.49 (d, *J* = 16.0 Hz, 1H, vinyl H), 7.43 (d, *J* = 15.9 Hz, 1H, vinyl H), 7.37 (td, *J* = 7.4, 1.6 Hz, 2H, H-3′, 5′), 7.27 (tt, *J* = 7.4, 1.0 Hz, 1H, H-4′), 7.11 (dd, *J* = 8.3, 1.9 Hz, 1H, H-6″), 7.06 (d, *J* = 1.9 Hz, 1H, H-2″), 6.86 (d, *J* = 8.3 Hz, 1H, H-5″), 6.74 (d, *J* = 15.2 Hz, 1H, vinyl H), 6.71 (d, *J* = 15.9 Hz, 1H, vinyl H), 6.65 (d, *J* = 8.5 Hz, 1H, H-5‴), 6.51 (d, *J* = 2.6 Hz, 1H, H-2‴), 6.35 (dd, *J* = 8.5, 2.6 Hz, 1H, H-6‴), 5.89 (s, 2H, OCH_2O), 3.91 (s, 3H, OCH_3), 3.90 (s, 3H, OCH_3), 2.49 (s, 3H, CH_3). ^{13}C-NMR (150 MHz, $CDCl_3$) δ: 188.63, 151.27, 150.80, 149.73, 149.22, 148.74, 147.60, 143.86, 142.69, 137.33, 131.06, 129.14, 127.81, 127.46, 124.58, 123.36, 122.90, 122.33, 111.05, 109.86, 108.28, 107.16, 105.79, 101.74, 98.20, 55.97, 55.92, 14.15. IR (KBr, cm^{-1}): 1668, 1616, 1506. ESI-MS m/z: 511.17 [M+H]$^+$, calcd for $C_{30}H_{26}N_2O_6$: 510.16.

(1E, 4E)-1-(5-(benzo[d][1,3]dioxol-6-yloxy)-3-methyl-1-phenyl-1H-pyrazol-4-yl)-5-(3,4,5-trimethoxyphenyl)penta-1,4-dien-3-one (7k)

A yellow solid, m.p:157.7–158.2°C, 16.8% yield. ^{1}H-NMR (600 MHz, $CDCl_3$), δ: 7.59 (dd, *J* = 8.7, 0.66 Hz, 2H, H-2′, 6′), 7.51 (d, *J* = 16.0 Hz, 1H, vinyl H), 7.39–7.36 (m, 3H, vinyl H, H-3′, 5′), 7.27 (t, *J* = 7.4 Hz, 1H, H-4′), 6.75 (s, 3H, H-2″, 6″, 2‴), 6.73 (d, *J* = 16.0 Hz, 1H, vinyl H), 6.64 (d, *J* = 15.9 Hz, 1H, vinyl H), 6.51 (d, *J* = 2.6 Hz, 1H, H-5‴), 6.35 (dd, *J* = 8.5, 2.6 Hz, 1H, H-6‴), 5.88 (s, 2H, OCH_2O), 3.88 (s, 6H, OCH_3), 3.87 (s, 3H, OCH_3), 2.49 (s, 3H, CH_3). ^{13}C-NMR (150 MHz, $CDCl_3$), δ: 188.53, 153.41, 150.78, 149.75, 148.74, 147.65, 143.86, 142.65, 140.24, 137.28,

131.41, 130.32, 129.15, 127.50, 125.94, 123.11, 122.32, 108.26, 107.15, 105.77, 105.45, 101.76, 98.17, 60.97, 56.18, 14.18. IR (KBr, cm^{-1}): 1667, 1622. ESI-MS m/z: 541.19 $[M+H]^+$, calcd for $C_{31}H_{28}N_2O_7$: 540.19.

(1*E*, 4*E*)-1-(5-(benzo[d][1,3]dioxol-6-yloxy)-3-methyl-1-phenyl-1*H*-pyrazol-4-yl)-5-(4-hydroxy-3-methoxyphenyl)penta-1,4-dien-3-one (7l)

A yellow solid, m.p:152.2–153.9°C, 10.7% yield. ^{1}H-NMR (600 MHz, $CDCl_3$), δ: 7.60 (d, *J* = 7.9 Hz, 2H, H-2′, 6′), 7.49 (d, *J* = 16.0 Hz, 1H, vinyl H), 7.41 (d, *J* = 16.0 Hz, 1H, vinyl H), 7.38 (t, *J* = 8.0 Hz, 2H, H-3′, 5′), 7.28 (t, *J* = 7.4 Hz, 1H, H-4′), 7.08 (dd, *J* = 8.1, 1.6 Hz, 1H, H-6″), 7.04 (s, 1H, H-2″), 6.92 (d, *J* = 8.2 Hz, 1H, H-5″), 6.74 (d, *J* = 16.0 Hz, 1H, vinyl H), 6.69 (d, *J* = 15.9 Hz, 1H, vinyl H), 6.66 (d, *J* = 8.5 Hz, 1H, H-5‴), 6.51 (d, *J* = 2.5 Hz, 1H, H-2‴), 6.35 (dd, *J* = 8.5, 2.6 Hz, 1H, H-6‴), 5.90 (s, 2H,OCH_2O), 5.88 (s, 1H, Ar-OH), 3.93 (s, 3H, OCH_3), 2.50 (s, 3H, CH_3). ^{13}C NMR (150 MHz, $CDCl_3$), δ: 188.72, 150.77, 149.76, 148.74, 148.15, 147.58, 146.81, 143.87, 142.94, 137.31, 131.05, 129.15, 127.48, 127.37, 124.28, 123.34, 123.26, 122.34, 114.77, 109.64, 108.29, 107.13, 105.78, 101.75, 98.20, 55.95, 14.14. IR (KBr, cm^{-1}): 3334, 1647, 1592. ESI-MS m/z: 597.17 $[M+H]^+$, calcd for $C_{29}H_{24}N_2O_6$: 496.16.

(1*E*, 4*E*)-1-(5-ethoxy-3-methyl-1-phenyl-1*H*-pyrazol-4-yl)-5-(4-hydroxy-3-methoxyphenyl) penta-1,4-dien-3-one (7m)

A yellow solid, m.p:157.3–157.7°C, 12.6% yield. ^{1}H NMR (600 MHz, $CDCl_3$) δ: 7.69 (d, *J* = 8.3 Hz, 2H, H-2′, 6′), 7.64 (d, *J* = 15.8 Hz, 2H, vinyl H), 7.45 (t, *J* = 7.7 Hz, 2H, H-3′, 5′), 7.32 (t, *J* = 7.4 Hz, 1H, H-4′), 7.17 (d, *J* = 8.2 Hz, 1H, H-6″), 7.11 (s, 1H, H-2″), 6.94 (d, *J* = 7.8 Hz, 1H, H-5″), 6.92 (d, *J* = 15.5 Hz, 1H, vinyl H), 6.86 (d, *J* = 15.5 Hz, 1H, vinyl H), 5.88 (s, 1H, Ar-OH), 4.04 (q, *J* = 7.0 Hz, 2H, OCH_2), 3.95 (s, 3H, OCH_3), 2.45 (s, 3H, CH_3), 1.30 (t, *J* = 6.9 Hz, 3H, CH_3).^{13}C NMR (150 MHz, $CDCl_3$) δ: 188.71, 153.09, 149.07, 148.11, 146.81, 142.79, 137.95, 132.64, 129.13, 127.50, 127.19, 124.16, 123.25, 122.41, 122.39, 114.81, 109.74, 104.75, 71.27, 55.97, 15.34, 14.41. IR (KBr, cm^{-1}): 1619, 1593. ESI-MS m/z: 405.18 $[M+H]^+$, calcd for $C_{24}H_{24}N_2O_4$: 404.17.

(1*E*, 4*E*)-1-(3, 4, 5-trimethoxyphenyl)-5-(1-methyl-1*H*-pyrazol-4-yl) penta-1, 4-dien-3-one (7n)

A yellow solid, m.p:111.2–111.7°C, 12.8% yield. ^{1}H NMR (600 MHz, $CDCl_3$), δ: 7.78 (s, 1H,Pyrazole-H), 7.62 (d, *J* = 15.8 Hz, 1H, vinyl H), 7.60 (s, 1H,Pyrazole-H), 7.59 (d, *J* = 15.8 Hz, 1H, vinyl H), 6.89 (d, *J* = 15.9 Hz, 1H, vinyl H), 6.83 (d, *J* = 16.1 Hz, vinyl H), 6.81 (s, 2H, ArH), 3.91 (s, 3H, NCH_3), 3.89 (s, 6H, OCH_3), 3.87 (s, 3H, OCH_3). ^{13}C-NMR (150 MHz, $CDCl_3$), δ: 188.50, 153.42, 142.79, 140.21, 138.81, 133.77, 130.93, 130.33, 125.08, 123.21, 118.95, 105.44, 60.97, 56.15, 39.21. IR (KBr, cm^{-1}): 1669, 1621. ESI-MS m/z: 329.15 $[M+H]^+$, calcd for $C_{18}H_{20}N_2O_4$: 328.14.

(1*E*, 4*E*)-1-(4-hydroxy-3-methoxyphenyl)-5-(1-methyl-1*H*-pyrazol-4-yl) penta-1, 4-dien-3-one (7o)

A yellow solid, m.p:153.3–153.5°C, 14.1% yield. ^{1}H NMR (600 MHz, $CDCl_3$), δ 7.77: (s, 1H,Pyrazole-H), 7.63 (d, *J* = 15.8 Hz, 1H, vinyl H), 7.61 (d, *J* = 15.9 Hz, 1H, vinyl H), 7.59 (s, 1H,Pyrazole-H), 7.15 (dd, *J* = 8.2, 1.7 Hz, 1H, H-6′), 7.09 (d, *J* =1.7 Hz, 1H, H-2′), 6.93 (d, *J* = 8.2 Hz, 1H, H-5′), 6.85 (d, *J* = 15.8 Hz, 1H, vinyl H), 6.82 (d, *J* = 15.8 Hz, 1H, vinyl H), 5.91 (s, 1H, Ar-OH), 3.94 (s, 3H, NCH_3), 3.92 (s, 3H, OCH_3). ^{13}C NMR (150 MHz, $CDCl_3$), δ: 188.67, 148.19, 146.84, 143.07, 138.80, 133.40, 130.83, 127.38, 123.42, 123.34, 119.02, 114.84, 109.69, 55.94, 39.19. IR (KBr, cm^{-1}): 1667, 1617. ESI-MS m/z: 285.12 $[M+H]^+$, calcd for $C_{16}H_{16}N_2O_3$: 284.11.

Biology

Cell Culture and Reagents

The human cancer cell lines SGC-7901, HepG2, A549, SW620 and human normal colon epithelial cells HCoEpiC were purchased from the Cell Collection Center of Wuhan University and maintained in Gibco RPMI medium 1640 (Gibco Company, Grand Island, NY, USA) supplemented with 10% fetal bovine serum (Gibco Company, Grand Island, NY, USA), 1% penicillin and streptomycin in a 5% CO_2 atmosphere at 37°C. Curcumin was purchased from Sigma Company (C1386, Sigma-Aldrich Chemical Company, Louis, Missouri, USA). Compound **7h** and curcumin were, respectively, dissolved in DMSO at 20 mM, which were then diluted to different concentrations in the prepared medium. Primary antibodies against ATM (2873, Cell Signaling Technology, Trask Lane Danvers, MA, USA), PARP (9542, Cell Signaling Technology, Trask Lane Danvers, MA, USA), cyclin B1 (sc-7393, Santa Cruz Biotechnology, Delaware Ave Santa Cruz, CA, USA), cyclin D1 (sc-6283, Santa Cruz Biotechnology, Delaware Ave Santa Cruz, CA, USA), CC3 (9662, Cell Signaling Technology, Trask Lane Danvers, MA, USA), Bcl-2 (ab196495, Abcam Inc., Cambridge, MA, USA),

plus all secondary antibodies, were obtained from Thermo (Thermo Fisher Scientific, Waltham, MA, USA).

Cell Viability Assay

A MTT assay was performed to assess cell viability according to the instructions of the manufacturer (Sigma-Aldrich Chemical Company, Louis, Missouri, USA). Briefly, 1×10^4 SW620 cells were plated onto 96-well plates. After cultured overnight, the cells were treated with different concentrations of **7h** and curcumin (0, 0.5, 1.25, 2.5, 5, 10 and 20 μM) for 24 h, 48 h and 72 h. At the end of each treatment, 20 μL of MTT (5 mg/mL) was added. After incubation for 4 h, the medium was carefully discarded and dimethyl sulfoxide (100 μL) was added. Absorbance was recorded at a wavelength of 490 nm by a Universal Microplate Reader (Bio-Tek Instruments, Winooski, USA), using a blank well as control. Cell viability and IC_{50} values of compounds for the four cancer cell lines were determined by comparison with control. Each experiment was repeated at least 3 independent times.

Transfection

SW620 cells were seeded into 6-well plates and transfected with Atm CRISPR Activation Plasmid (sc-400,192-ACT, Santa Cruz Biotechnology, Delaware Ave Santa Cruz, California, USA) and lipofectamine 2000 (Invitrogen Inc., Carlsbad, CA, USA) by following the manufacture's instruction. After the indicated periods of incubation, the cells were subjected to further analysis.

Transwell Migration and Invasion Assay

For transwell migration assays, 1×10^6 cells were plated into the top chamber of a transwell (Corning, Acton, MA, USA) with a porous membrane (8.0-μm pore size). Then, the cells were plated in medium with minimal serum (0.5% FBS), and medium supplemented with additional serum (10% FBS) was used to produce a chemoattractant effect in the lower chamber. Compound **7h** at different concentrations was added. The cells were incubated for 24 h at 37°C and cells that did not migrate through the pores were removed using a cotton swab. Cells on the lower surface of the membrane were stained with crystal violet (Sigma-Aldrich Chemical Company, Louis, Missouri, USA). The migrated cells were manually quantified. The inhibition rates of migrated cells were calculated using the untreated group as 100%.

As for in vitro cellular invasion analysis, briefly, 1×10^6 cells in serum-free medium were seeded into the upper chamber of an insert coated with Matrigel. Medium supplemented with 10% FBS was placed over the lower chamber and then **7h** at different concentrations were added. After incubation for 24 h, the upper layer of cells was removed by cotton wool. The cells on the lower surface were fixed in methanol and stained with 0.1% crystal violet, and then imaged using an IX71 inverted microscope (Olympus, Tokyo, Japan). The number of migrating cells in a total of five randomly selected fields was counted. All experiments were performed in triplicate.

Clonogenic Assay

In order to examine the survival of cells treated with **7h**, SW620 cells were plated (1×10^6 per well) in a 6-well plate and incubated overnight. After exposure to different concentrations of **7h** for 48 h, the viable cells were counted and then seeded into 6-well plate in a density of 5,000 cells per well. The cells were then incubated for 14 days at 37°C in a humidified 5% CO_2 atmosphere. All the colonies were stained with 2% crystal violet and cells were counted manually.

Cell Apoptosis Analysis

The apoptotic cells were detected with an Annexin V-FITC/PI apoptosis detection kit (Biouniqure, Beijing, China) according to the manufacturers' instructions. Briefly, 1×10^6 SW620 cells were incubated in 6-well plate overnight and treated with various concentrations of **7h** and curcumin for 48 h. Cells were harvested by centrifugation, washed with PBS, then resuspended in 500 μL of binding buffer with 5 μL propidium iodide (PI) and kept in the dark for 5 min at room temperature. Next, 5 μL FITC-conjugated anti-Annexin V antibody was added, which was kept in the dark for 10 min at room temperature. Apoptosis was analyzed by a flow cytometer (Becton Dickinson, Mountain View, CA, USA).

Cell Cycle Analysis

Exponentially growing SW620 cells were seeded in a 6-well plate and incubated overnight. The cells were treated, respectively, with curcumin and **7h** and then cultured for 48 h. At the end of treatment period, cells were collected and fixed with ice-cold 75% (v/v) ethanol and kept at 4°C overnight. The cells were collected and washed with ice-cold PBS. Then, the cell pellets were resuspended at 1×10^6 cells/mL in PBS and incubated with 0.1 mg/mL RNase I and 50 mg/mL Propidium iodide (PI) at 37°C for 30 min. DNA contents were determined with a flow cytometer (Becton Dickinson, Mountain View, CA, USA).

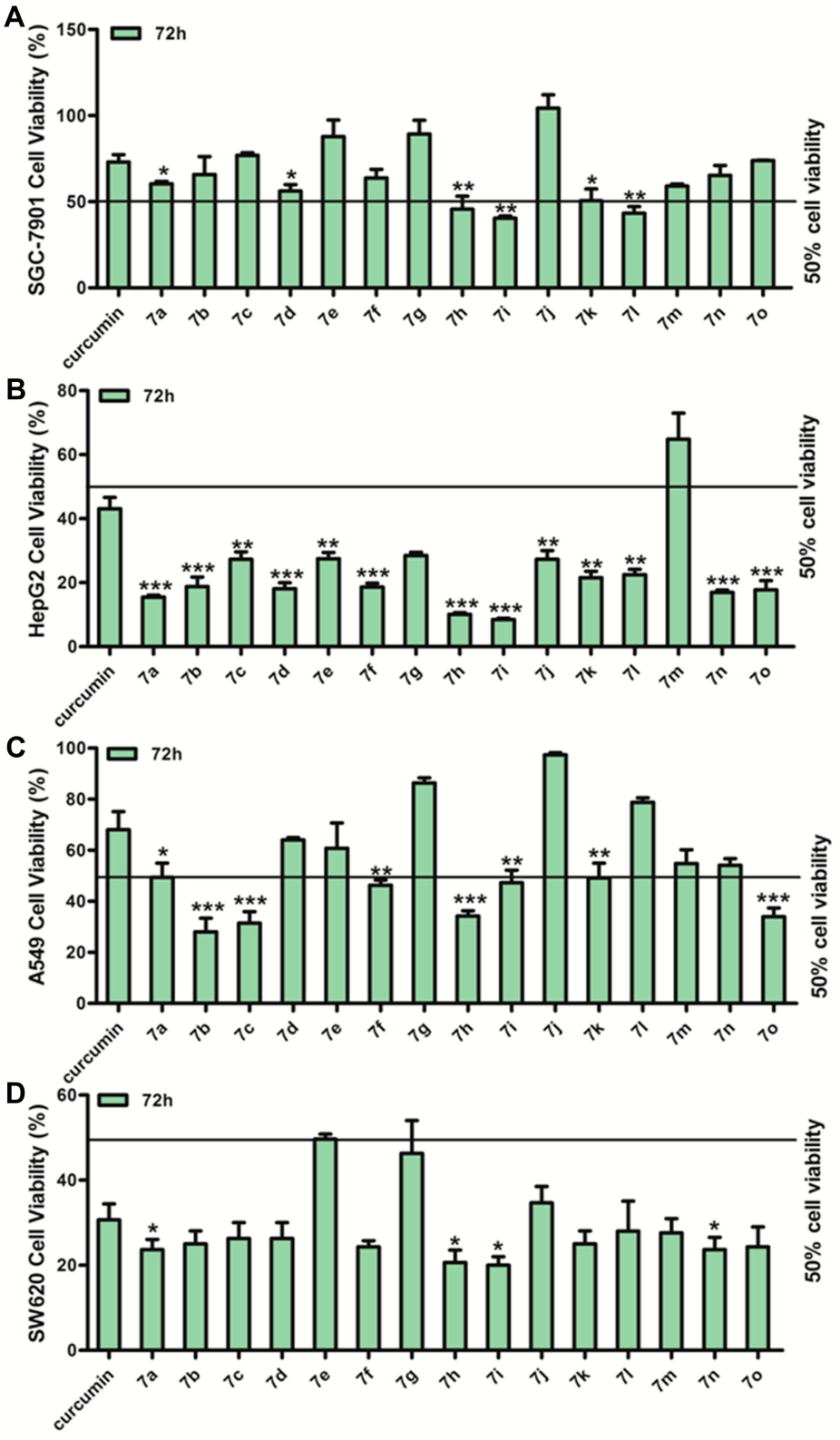

Figure 2 The inhibitions of cell viability for the synthesized compounds (7a–7o) on human cancer cell lines SGC-7901 (**A**), HepG2 (**B**), A549 (**C**) and SW620 (**D**). The cells were treated with 7a-7o (20 μM) for 72 h, and then the cell viability was determined by MTT assay, curcumin as positive control. Results were presented as Mean±S.D (n=3) and analyzed by GraphPad Prism 6.0 followed by the Student *t*-test. *P < 0.05, **p< 0.01 or ***p < 0.001 vs curcumin.

Table 1 The IC_{50} Value of Inhibiting Proliferation of the Various Cancer Lines Treated with Compounds 7a, 7h, 7i After 24 h, 48 h, 72 H.

Compound	IC_{50} (μM)											
	SGC7901			HepG2			A549			SW620		
	24h	48h	72h	24h	48h	72h	24h	48h	72h	24h	48h	72h
Curcumin	31.51±0.04	18.91±0.39	11.40±1.80	16.01±0.83	14.89±0.38	12.79±0.51	21.04±0.93	15.43±1.43	12.49±0.15	46.88±2.45	14.36±0.95	9.36±1.48
Adriamycin	9.92±0.54	2.53±0.33	1.64±0.17	13.17±0.51	6.78±0.31	5.70±0.43	16.93±1.09	5.78±1.41	3.01±0.21	24.34±0.61	3.48±1.31	3.28±0.34
7a	43.99±1.48	19.86±0.65	5.18±0.24***	46.92±4.11	12.61±2.39	3.22±0.76***	28.10±2.41	19.83±0.79	10.50±1.01	14.36±0.95***#	2.25±0.28***	1.67±0.33***##
7h	9.94±0.50***	1.77±0.24***	1.66±0.07***	83.21±2.11	3.20±0.04***##	2.12±0.07***###	24.83±1.79	3.31±0.05***#	2.61±0.28***	19.81±1.15***#	1.41±0.18***##	0.012±0.008***###
7i	26.04±3.40*	5.24±0.23***	1.69±0.30***	13.25±1.76	4.697±1.24***#	4.96±1.08***#	30.23±1.79	5.50±0.47***	4.62±0.79***	16.70±0.81***#	3.39±0.20***	0.27±0.01***###

Notes: Results were presented as Mean ± SD (n = 3) and analyzed by GraphPad Prism 6.0 followed by the Student t-test. *p < 0.05 or ***p < 0.001 vs Curcumin, #P < 0.05, ##P < 0.01 or ###P < 0.001 vs Adriamycin.

Western Blot Analysis

The expressions of several proteins were detected by Western blot analysis. The SW620 cells were treated, respectively, with **7h**, Atm CRISPR Activation Plasmid, **7h**+ Atm CRISPR Activation Plasmid. The harvested SW620 cells were washed by PBS and lysed with cell lysis buffer (Cell Signaling, Danvers, MA, USA). The protein concentrations were tested by a BCA Protein Assay kit (Thermo Fisher Scientific, Waltham, MA, USA). Equal amounts of protein samples were prepared and fractionated by electrophoresis in a sodium dodecyl sulfonate-polyacrylamide gel and transferred onto a polyvinylidene fluoride membrane. Skimmed milk powder was added, and the samples were incubated for 2 h. Next, appropriate primary antibodies were added, and the sample was finally incubated at 4°C overnight. The membranes were incubated for 1 h with secondary antibodies at room temperature and then washed three times with tris-buffered saline and Tween 20. Protein bands were subsequently detected by electrogenerated chemiluminescence assay.

Statistical Analysis

All data analyses were conducted using IBM SPSS, Version 19.0 (IBM Corp., Armonk, NY, USA). Statistical comparisons were performed using the Student *t*-test. P-values < 0.05 were considered statistically significant. Results were expressed as means ± standard deviations.

Results and Discussion

Synthesis of MCACs

The condensation of phenylhydrazine with ethyl acetoacetate afforded 1-phenyl-3-methyl-5-pyrazolone **9**, which was followed by the Vilsmeier reaction to produce 5-chloro-3-methyl-1-phenyl-1*H*-pyrazole-4-carbaldehyde **10**. Compound **10** was treated with ethanol or substituted phenols in the presence of KOH to give substituted 1*H*-pyrazole-4-carbaldehydes **11a–11c**. Various substituted benzaldehydes conducted the Claisen-Schmid condensation with acetone in the presence of 10%NaOH to furnish α, β-unsaturated ketones **13a–13f**. Using the same NaOH-catalysed Claisen-Schmidt condensations of **13a–13f** with **10, 11a–11c** or 1-methyl-1*H*-pyrazole-4-carbaldehyde, the target compounds **7a**–**7o** were finally obtained. All the target compounds **7a**–**7o** were well characterized by spectroscopic techniques such as IR, NMR and ESI-MS, which were in full accordance with the depicted structures. The

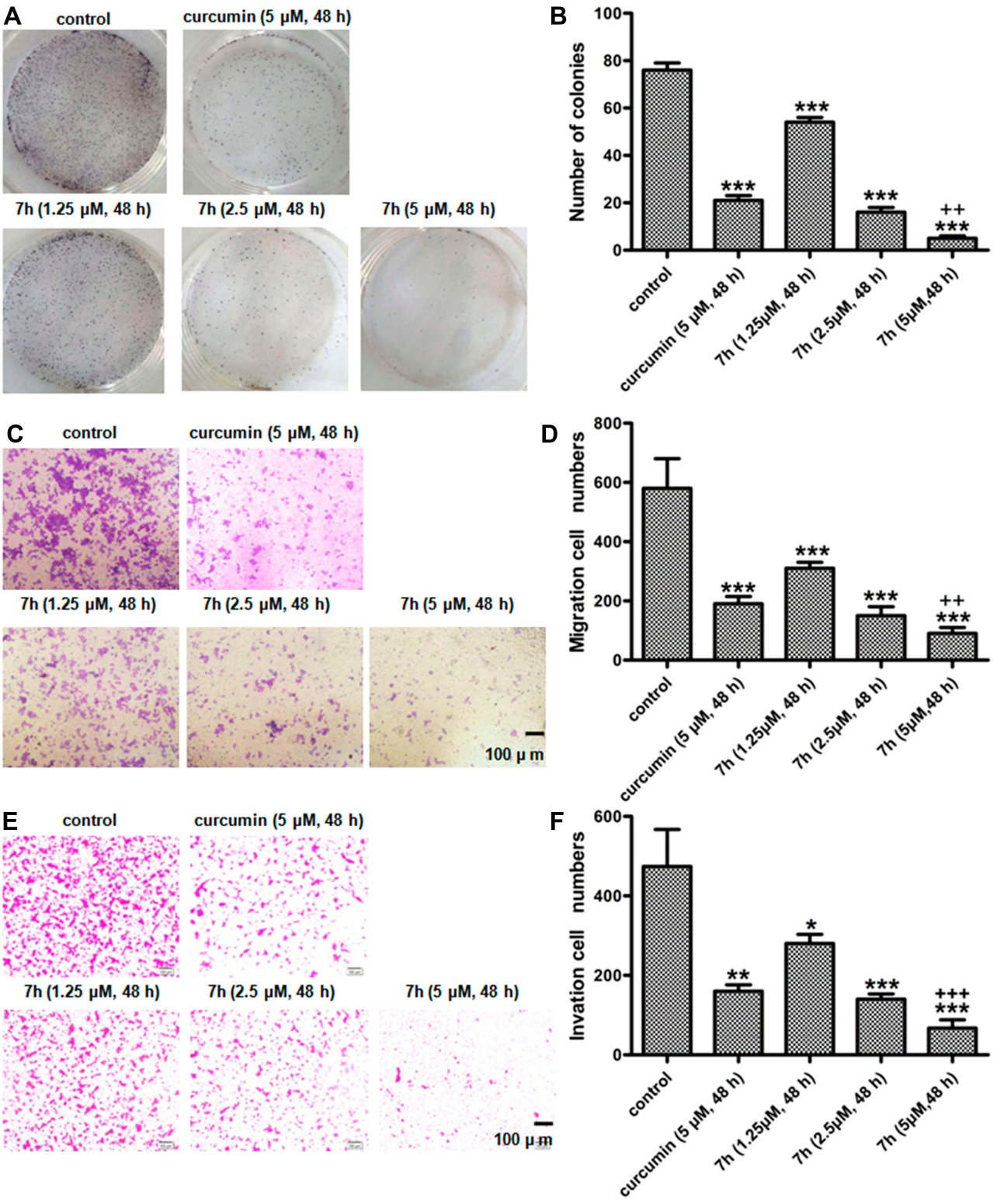

Figure 3 Compound 7h inhibited clone formation (**A** and **B**), migration (**C** and **D**) and invasion (**E** and **F**) on SW620 cells. SW620 cells were treated with 7h at the concentration of 1.25 μM, 2.5 μM and 5 μM for 48h respectively, the cells treated with DMSO as control and with curcumin (5 μM) as positive control. Results were presented as Mean ± SD (n = 3) and analyzed by GraphPad Prism 6.0 followed by the Student *t*-test. $^{*}P < 0.05$ or $^{**}P < 0.01$ or $^{***}P < 0.001$ vs control, $^{++}P < 0.01$ or $^{+++}P < 0.001$ vs curcumin.

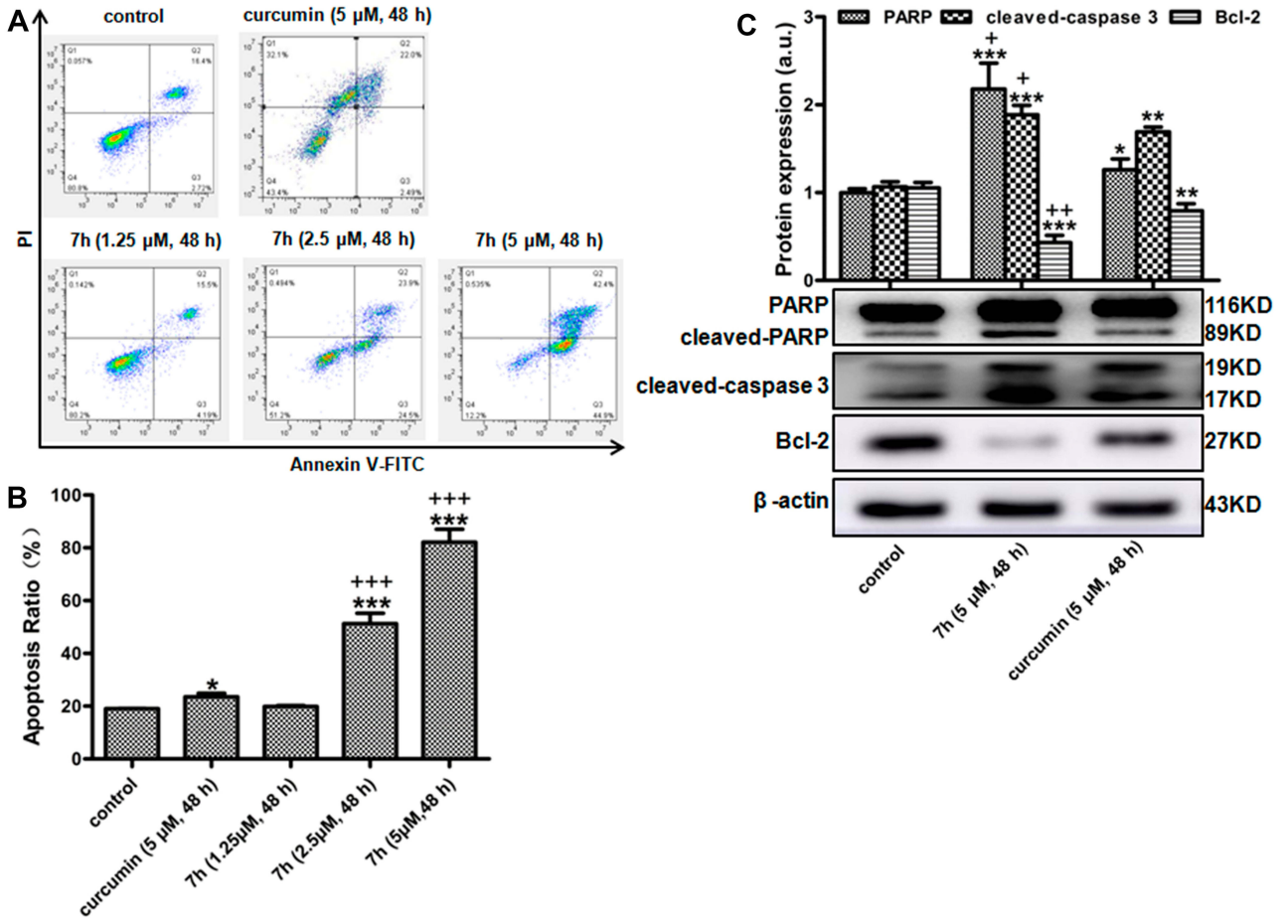

Figure 4 The effect of 7h on apoptosis in SW620 cells. SW620 cells were treated with 7h (1.25, 2.5 or 5 μM) for 48 h, and the cell apoptotic rate was detected with FCM assay (**A** and **B**), the cells with DMSO as control and with curcumin (5 μM) as positive control. (**C**) The effects of 7h on the protein expression of PARP, cleaved-caspase 3 and Bcl-2 were tested by Western blot. Data were presented as Mean ± SD (n = 3) and analyzed by GraphPad Prism 6.0 followed by the Student *t*-test. *P < 0.05, **P < 0.01 or ***P < 0.001 vs control, $^{+}$P < 0.05, $^{++}$P < 0.01 or $^{+++}$P < 0.001 vs curcumin.

proton NMR of **7a**–**7o** exhibited two pair of doublets in the aromatic region with *J* values between 15.5 and 16.1 Hz for the alkene protons present in the penta-1, 4-dien-3-one skeleton, providing evidence of (*E*)-stereochemistry. Before used for biological assays, all synthesized compounds **7a**–**7o** were determined their purity (all >97%) by HPLC.

Effect of the Synthesized Compounds on Cell Viability

The inhibitory effects of the synthesized compounds on the proliferation of human cancer cell lines GC-7901, HepG2, A549 and SW620 were assessed by MTT assay at a concentration of 20μM respectively, and curcumin was used as positive control. The results indicated that most of the synthesized compounds decreased cell viability significantly as compared to curcumin, especially after 72 h when HepG2, A549 and SW620 cells were treated with these synthesized compounds (Figure 2). Among them, compounds **7a, 7h** and **7i** exhibited excellent inhibitory activities, especially in SW620 cells with the ratio of cell viability <50%. Further, the IC_{50} values of compounds **7a, 7h, 7i** were determined at the time of 24h, 48h and 72h, respectively, and curcumin, adriamycin and oxaliplatin were used as positive control. The results are shown in Table 1. Compound **7h** exhibited more potent inhibitory activity against SW620 cells with IC_{50} value of 0.012 μM than the three positive controls. Furthermore, in order to evaluate its cytotoxicity to normal cells, **7h** was chosen to test its inhibitory effects on the proliferation of human normal colon epithelial cells HCoEpiC at the time of 72 h, and the IC_{50} value was more than 100μM, implying that **7h** exhibited selective cytotoxicity to cancer cells. The preliminary study on structure–activity relationship (SAR), taking that in

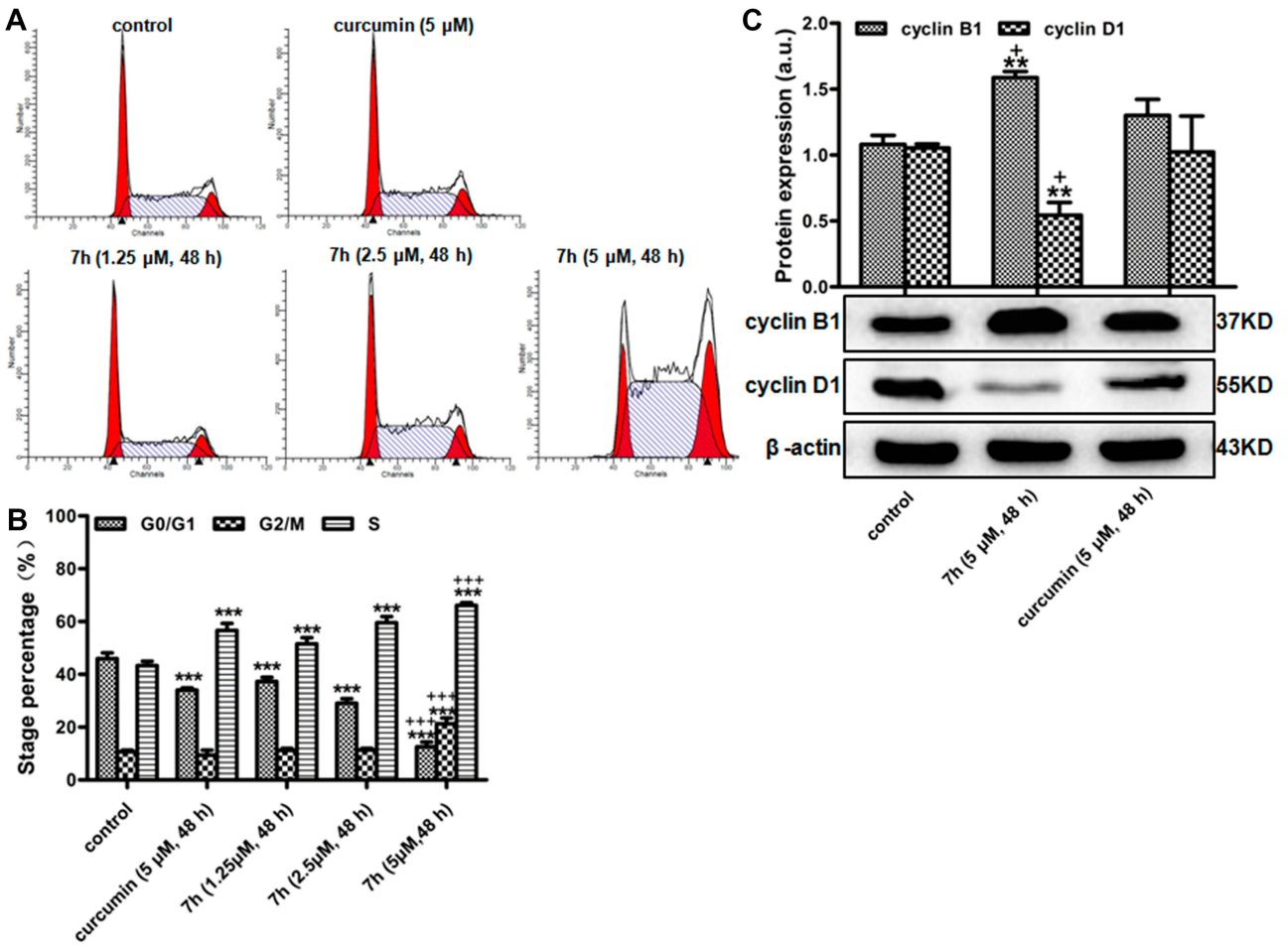

Figure 5 The effect of 7h on cell cycle. (**A** and **B**) SW620 cells were treated with 7h (1.25, 2.5 or 5 μM) for 48 h, and then the cell cycle distribution was detected by PI staining, the cells with DMSO as control and with curcumin (5 μM) as positive control. (**C**) Western blotting was used to detect the expression of cyclin B1 and cyclin D1 protein. Data were presented as Mean ± SD (n = 3) and analyzed by GraphPad Prism 6.0 followed by the Student *t*-test. **P < 0.01 or ***P < 0.001 vs control, $^{+}$P < 0.05 or $^{++}$P < 0.001 vs curcumin.

SW620 cells as an example, indicated that on the terminal containing pyrazolyl ring of these MCACs ethoxy or phenoxy groups resulted in better activity than chlorine atom. Excepted for **7g**, 2-methoxyphenoxy group was introduced into **7h, 7i** to replace the chlorine atom, which showed the most potent activity. On another terminal of these MCACs, trimethoxyphenoxy (3, 4, 5-OCH_3) group together with both 3-methoxy and 4-hydroxyl groups might contribute to good activities.

Effect of 7h on Migration and Colony Formation in SW620 Cells

The migration and invasion of cancer cells due to their promoted penetration into the lymphatic system and blood vessels can lead to metastasis dissemination, and then cancer cells undergo extravasation into a newly metastatic site where they proliferate.[33] Thus, an ability to inhibit the migration and invasion of cancer cells is very important for an anticancer compound. As **7h** exhibited excellent inhibitory activities against the proliferation of SW620 cancer cells, further, its effects on inhibitions of the migration and colony formation of SW620 cells were evaluated at the various concentrations of 1.25μM, 2.5μM and 5μM after the cells were treated with **7h** for 48 h. The cells treated with DMSO and curcumin (5 μM) were used as blank and positive control correspondingly. The results indicated that **7h** decreased the number of migration and invasion in a dose-dependent manner (Figure 3A–D), and there was a significant reduction in the percentages of cell migration and invasion especially at the concentration of 5μM as compared with both control groups. As shown in Figure 3E and F, the clonogenic quantity of

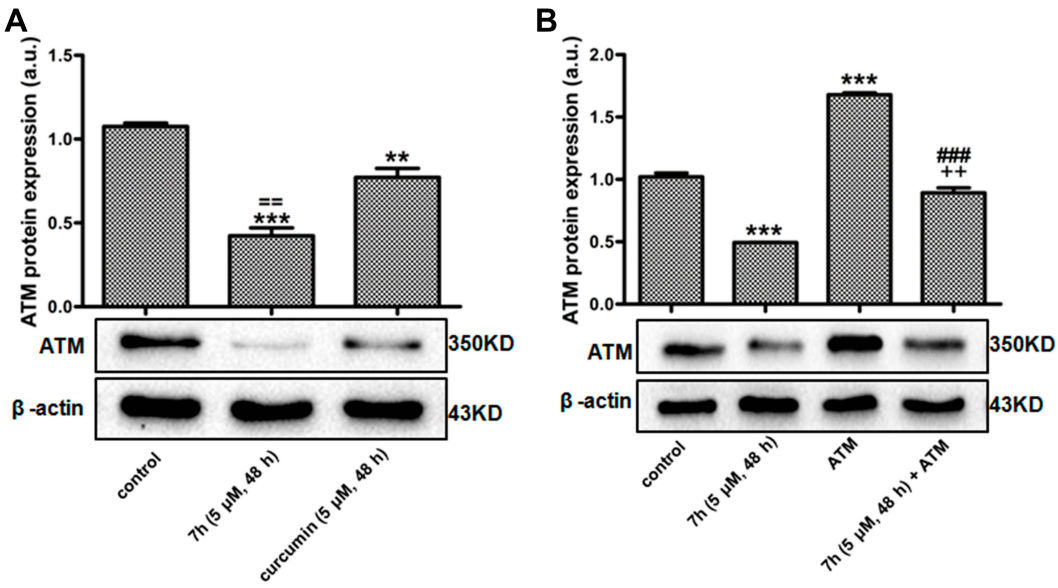

Figure 6 Compound 7h down-regulated ATM protein expression in SW620 cells. (**A**) SW620 cells were treated with curcumin (5 μM) and 7h (5 μM) for 48 h, and then ATM protein expression was detected, the cells were treated with DMSO as control group; (**B**) SW620 cells were treated with ATM plasmid (Atm CRISPR Activation) for 24 h and then combined with or without 7h for 48 h, and the cells with negative plasmid as control. Data were presented as Mean ± SD (n = 3) and analyzed by GraphPad Prism 6.0 followed by the Student *t*-test. $^{**}P < 0.01$ or $^{***}P < 0.001$ vs control, $^{++}P < 0.01$ vs compound 7h, $^{\#\#\#}P < 0.001$ vs ATM, $^{==}P < 0.01$ vs curcumin.

SW620 cells treated with **7h** (5μM) decreased nearly by thirteen-fold as compared to the positive control. These results indicated that **7h** could significantly inhibit cell proliferation.

Effect of 7h on SW620 Cell Apoptosis

In order to evaluate the effect of **7h** on cell apoptosis, SW620 cells were treated with **7h** at the concentrations of 1.25μM, 2.5μM and 5μM for 48 h, respectively, and then the apoptosis was analyzed by flow cytometry, using the cells treated with DMSO and curcumin (5 μM) as blank and positive control correspondingly. The results (Figure 4A and B) showed that the treatment with **7h** increased the apoptotic rate from 18.64% of vehicle control to 19.69% (1.25 μM), 47.4% (2.5 μM) and 87.3% (5 μM) in a concentration-dependent manner. Compared to curcumin group, **7h** significantly increased the cell apoptotic rate at the concentration of 2.5μM and 5μM. On the other hand, Western blotting result (Figure 4C) showed that **7h** markedly increased the protein expression of cleaved-caspase 3 and PARP and decreased Bcl-2 expression at the concentration of 5μM in SW620 cells as compared with curcumin (5μM) group, which suggested that **7h** promoted SW620 cell apoptosis.

Effect of 7h on SW620 Cell Cycle

SW620 cells were treated with **7h** at the concentrations of 1.25μM, 2.5μM and 5μM for 48h, respectively, and then the cell cycle was determined, the cells treated with DMSO as control and curcumin (5μM) as positive control. As shown in Figure 5A and B, compound **7h** at the concentration of 5μM increased the percentages of G2/M phase cells from 10% to 21% and that of S phase cells from 43% to 66%, while decreased the percentages of G0/G1 phase cells from 46% to 11%. Compared to the control and the positive control group, compound **7h** significantly increased the percentages of G2/M phase cells at the concentration of 5μM. The results indicated that **7h** inhibited SW620 cell proliferation by inducing cell cycle arrest at G2/M and S phase. Meanwhile, the expressions of cyclin B1 and cyclin D1 were also determined by Western blot assay, and the results (Figure 5C) showed that **7h** increased cyclin B1 protein expression and decreased cyclin D1 protein expression at the concentration of 5μM in SW620 cells.

Compound 7h Regulated ATM Expression on SW620 Cells

The ATM gene is a DNA repair gene and is located on the chromosome llq22-q23. Studies have shown that the ATM gene may become a new potential target for the treatment of colon cancer,[34] and then we hypothesized that the inhibitory effect of **7h** on the proliferations of SW620 cells might be related to ATM pathway. Therefore, SW620 cells were treated with **7h** (5μM) and curcumin (5μM) for 48 h, and then ATM protein expressions were determined, the cells treated with DMSO as control. The

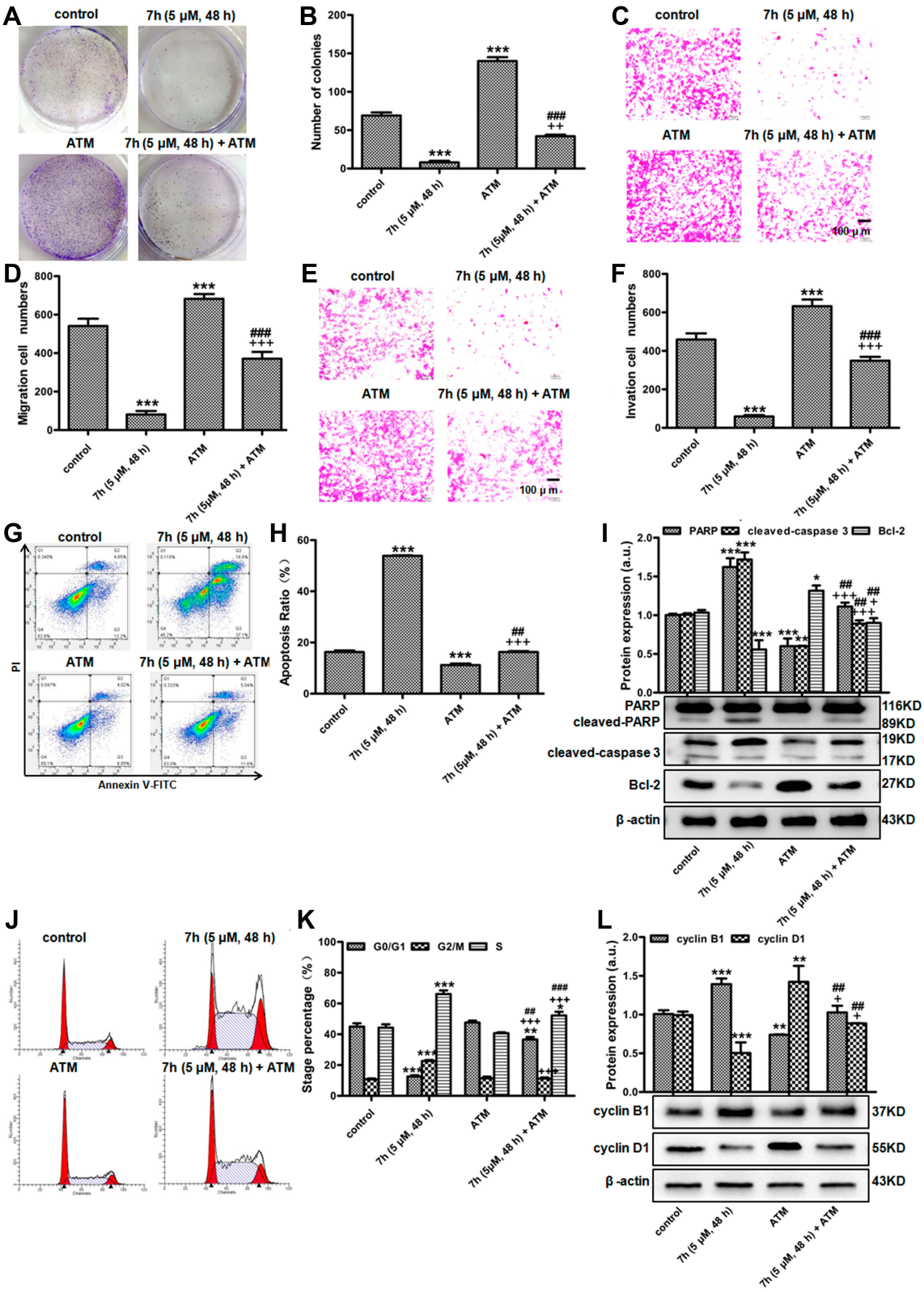

Figure 7 The effects of 7h on apoptosis, cell cycle, migration and invasion were partly dependent on ATM pathway in SW620 cells. SW620 cells were transfected with ATM plasmid (Atm CRISPR Activation) for 24 h and then combined with or without 7h for 48 h, and the cells were treated with negative plasmid as control. The clone formation (**A** and **B**) and cell migration and invasion (**C**–**F**) were detected; The apoptotic rate and apoptotic relative protein expression (**G**–**I**) were detected by FCM and Western blot assay; The cell cycle arrest, cell cycle arrest-related protein expression (**J**–**L**) were also detected. Results were presented as Mean ± SD (n = 3) and analyzed by GraphPad Prism 6.0 followed by the Student *t*-test. $^{*}P < 0.05$, $^{**}P < 0.01$ or $^{***}P < 0.001$ vs control, $^{+}P < 0.05$, $^{++}P < 0.01$ or $^{+++}P < 0.001$ vs compound 7h, $^{\#\#}P < 0.01$ or $^{\#\#\#}P < 0.001$ vs ATM.

Western blotting results revealed that **7h** markedly decreased ATM protein expression as compared to both control and curcumin (5μM) groups (Figure 6A). Further, in order to confirm whether **7h** could really down-regulated ATM signal, SW620 cells were transfected with the ATM activated plasmids that over-expressed ATM protein for 24 h. The cells were treated with **7h** for 48 h, using the cells treated with negative plasmids as control. The result showed that the ATM activated plasmids reversed the down-regulation of ATM expression induced by **7h** (Figure 6B), which also proved that **7h** decreases the ATM protein expression in SW620 cells.

Effects of 7h on Cell Apoptosis, Cycle, Migration and Invasion in SW620 Cells Were Partly via ATM Pathway

As **7h** decreased the ATM protein expression, in order to investigate whether its effects on SW620 cells migration, invasion, cell cycle and apoptosis were via ATM pathway, the related assays were performed, and SW620 cells were transfected with or without ATM activated plasmids were used for comparison. The cells were treated with **7h** (5μM), using the cells with negative plasmids as control. The result demonstrated that the transfection with ATM activated plasmids could reverse the up-regulation of the apoptotic rate induced by **7h** (Figure 7G and H). Similarly, the Western blotting result indicated that the expressions of cleaved-caspase 3, PARP and Bcl-2 induced by **7h** in SW620 cells were all decreased by **7h** combined with ATM activated plasmid (Figure 7I). Meanwhile, the treatment with **7h**+ATM significantly restored cell cycles that were obviously different from the ones induced only by **7h** (Figure 7J and K). Correspondingly, **7h**+ATM clearly reduced the up-regulation of cyclin B1 protein expression while enhanced the protein expression of cyclin D1 as compared to treatment only with **7h** (Figure 7L). Finally, the present study also demonstrated that **7h**+ATM significantly enhanced the decline of the migration and invasion number induced only by **7h** (Figure 7C–F). Although **7h** decreased the amount of clone formation, the amount was drastically increased from 1.33 ± 1.01 to 8.22 ± 2.22 after treatment with **7h**+ATM for 48 h(Figure 7A and B). In brief, the treatment combined **7h** with ATM protein could almost reverse all the effects resulted only from **7h**, which suggested that **7h** exerted its activities, such as induction of cell apoptosis, cycle arrest, migration and clone formation inhibitions, possibly due to its ability to decrease the ATM expression in SW620 cells.

Conclusion

A serial of monocarbonyl analogs of curcumin containing pyrazole moiety was designed and synthesized whose structures were confirmed by spectroscopic techniques. Their inhibitory activities against four human cancer lines, SGC-7901, HepG2, A549 and SW620, were evaluated. Of these 15 newly synthesized compounds, (1*E*,4*E*)-1-(5-(2-methoxyphenoxy)-3- methyl-1-phenyl-1*H*-pyrazol-4-yl)-5-(3, 4, 5-trimethoxyphenyl) penta-1, 4-dien-3-one **7h** exhibited excellent selectivity and outstanding anti-proliferation activity against SW620 cells with a IC_{50} value of 12 nM, which was more potent than curcumin (IC_{50} = 9.36 μM), adriamysin (IC_{50} = 3.28 μM) and oxaliplatin (IC_{50} = 13.33 μM).

In order to investigate the mechanisms that **7h** exerted its inhibitory effect on SW620 cells proliferation, further assays were performed. The results showed that **7h** inhibited cell migration, invasion and colony formation of SW620 colon cancer cells obviously, which was due to its ability to induce cell cycle arrest in the G2/M and S phases and apoptosis. Ultimately, **7h** decreased the expression of ATM protein, which may primarily contribute to its anticancer activity against SW620 cells. All the data indicated that **7h** could be identified and developed as a novel potential anti-colon cancer agent in the future.

Abbreviations

MCACs, monocarbonyl analogs of curcumin; MTT, methyl thiazolyl tetrazolium; IC_{50}, 50% inhibitory concentration; ATM, ataxia-telangiectasia mutated; PARP, poly ADP-ribose polymerase; CRISPR, clustered regularly interspaced short palindromic repeats; FBS, fetal calf serum.

Acknowledgment

The financial supports by the National Natural Science Foundation of China (No. 81770377) and the Natural Science Foundation of Hubei Province (No. 2017CFB448) is gratefully acknowledged.

Disclosure

The authors report no conflicts of interest in this work.

References

1. O'Keefe SJ. Diet, microorganisms and their metabolites, and colon cancer. *Nat Rev Gastro Hepat*. 2016;13(12):691–706.

2. Liu X, Wan X, Kan H, et al. Hypoxia-induced upregulation of Orai1 drives colon cancer invasiveness and angiogenesis. *Eur J Pharmacol*. 2018;832:1–10. doi:10.1016/j.ejphar.2018.05.008
3. Ji X, Peng Q, Wang M. Anti-colon-cancer effects of polysaccharides: a mini-review of the mechanisms. *Int J Biol Macromol*. 2018;114:1127–1133. doi:10.1016/j.ijbiomac.2018.03.186
4. Prasad S, Gupta SC, Tyagi AK, et al. Curcumin, a component of golden spice: from bedside to bench and back. *Biotechnol Adv*. 2014;32(6):1053–1064. doi:10.1016/j.biotechadv.2014.04.004
5. Nelson KM, Dahlin JL, Bisson J, et al. The essential medicinal chemistry of curcumin. *J Med Chem*. 2017;60(5):1620–1637. doi:10.1021/acs.jmedchem.6b00975
6. Baker M. Chemists warn against deceptive molecules. *Nature*. 2017;541:144–145. doi:10.1038/541144a
7. Padmanaban G, Nagaraj VA. Curcumin may defy medicinal chemists. *ACS Med Chem Lett*. 2017;8(3):274. doi:10.1021/acsmedchemlett.7b00051
8. Bahadori F, Demiray M. A realistic view on "the essential medicinal chemistry of curcumin". *ACS Med Chem Lett*. 2017;8(9):893–896. doi:10.1021/acsmedchemlett.7b00284
9. Kumar S, Kesharwani SS, Mathur H, et al. Molecular complexation of curcumin with pH sensitive cationic copolymer enhances the aqueous solubility, stability and bioavailability of curcumin. *Eur J Pharm Sci*. 2016;82:86–96. doi:10.1016/j.ejps.2015.11.010
10. Kesharwani SS, Ahmad R, Bakkari MA, et al. Site-directed non-covalent polymer-drug complexes for inflammatory bowel disease (IBD): formulation development, characterization and pharmacological evaluation. *J Control Release*. 2018;290:165–179. doi:10.1016/j.jconrel.2018.08.004
11. Jalde SS, Chauhan AK, Lee JH, et al. Synthesis of novel Chlorin e6-curcumin conjugates as photosensitizers for photodynamic therapy against pancreatic carcinoma. *Eur J Med Chem*. 2018;147:66–76. doi:10.1016/j.ejmech.2018.01.099
12. Khwaja S, Fatima K, Hasanain M, et al. Antiproliferative efficacy of curcumin mimics through microtubule destabilization. *Eur J Med Chem*. 2018;151:51–61. doi:10.1016/j.ejmech.2018.03.063
13. Hampannavar GA, Karpoormath R, Palkar MB, et al. An appraisal on recent medicinal perspective of curcumin degradant: dehydrozingerone (DZG). *Bioorg Med Chem*. 2016;24(4):501–520. doi:10.1016/j.bmc.2015.12.049
14. Mock CD, Jordan BC, Selvam C. Recent advances of curcumin and its analogues in breast cancer prevention and treatment. *RSC Adv*. 2015;5(92):75575–75588. doi:10.1039/C5RA14925H
15. Bairwa K, Grover J, Kania M, et al. Recent developments in chemistry and biology of curcumin analogues. *RSC Adv*. 2014;4(27):13946–13978. doi:10.1039/c4ra00227j
16. Liu GY, Zhai Q, Chen JZ, et al. 2, 2′-Fluorine mono-carbonyl curcumin induce reactive oxygen species-Mediated apoptosis in Human lung cancer NCI-H460 cells. *Eur J Pharmacol*. 2016;786:161–168. doi:10.1016/j.ejphar.2016.06.009
17. Ai Y, Zhu B, Ren C, et al. Discovery of new monocarbonyl Ligustrazine-Curcumin hybrids for intervention of drug-sensitive and drug-resistant lung cancer. *J Med Chem*. 2016;59(5):1747–1760. doi:10.1021/acs.jmedchem.5b01203
18. Mandalapu D, Singh DK, Gupta S, et al. Discovery of monocarbonyl curcumin hybrids as a novel class of human DNA ligase I inhibitors: in silico design, synthesis and biology. *RSC Adv*. 2016;6(31):26003–26018. doi:10.1039/C5RA25853G
19. Wang J, Wang X, Wang Y, et al. Novel curcumin analogue hybrids: synthesis and anticancer activity. *Eur J Med Chem*. 2018;156:493–509. doi:10.1016/j.ejmech.2018.07.013
20. Sri Ramya PV, Angapelly S, Guntuku L, et al. Synthesis and biological evaluation of curcumin inspired indole analogues as tubulin polymerization inhibitors. *Eur J Med Chem*. 2017;127:100–114. doi:10.1016/j.ejmech.2016.12.043
21. Chen L, Li Q, Weng B, et al. Design, synthesis, anti-lung cancer activity and chemosensitization of tumor-selective MCACs based on ROS-mediated JNK pathway activation and NF-kB pathway inhibition. *Eur J Med Chem*. 2018;151:508–519. doi:10.1016/j.ejmech.2018.03.051
22. Zhang Y, Liu Z, Wu J, et al. New MD2 inhibitors derived from curcumin with improved anti-inflammatory activity. *Eur J Med Chem*. 2018;148:291–305. doi:10.1016/j.ejmech.2018.02.008
23. Dong L, Zheng S, Zhang Y, et al. Design, synthesis, and evaluation of semiconservative mono-carbonyl analogs of curcumin as anti-inflammatory agents against lipopolysaccharide-induced acute lung injury. *Med Chem Commun*. 2015;6(8):1544–1553. doi:10.1039/C5MD00113G
24. Zhang Y, Zhao C, He W, et al. Discovery and evaluation of asymmetrical monocarbonyl analogs of curcumin as anti-inflammatory agents. *Drug Des Dev Ther*. 2014;8:373–382.
25. Deck LM, Hunsaker LA, Vander Jagt TA, et al. Activation of anti-oxidant Nrf2 signaling by enone analogues of curcumin. *Eur J Med Chem*. 2018;143:854–865. doi:10.1016/j.ejmech.2017.11.048
26. Chen QH, Yu K, Zhang X, et al. A new class of hybrid anticancer agents inspired by the synergistic effects of curcumin and genistein: design, synthesis, and anti-proliferative evaluation. *Bioorg Med Chem Lett*. 2015;25(20):4553–4556. doi:10.1016/j.bmcl.2015.08.064
27. Sri Ramya PV, Guntuku L, Angapelly S, et al. Curcumin inspired 2-chloro/phenoxy quinoline analogues: synthesis and biological evaluation as potential anticancer agents. *Bioorg Med Chem Lett*. 2018;28(5):892–898. doi:10.1016/j.bmcl.2018.01.070
28. Luo H, Yang S, Cai Y, et al. Synthesis and biological evaluation of novel 6-chloro-quinazolin derivatives as potential antitumor agents. *Eur J Med Chem*. 2014;84:746–752. doi:10.1016/j.ejmech.2014.07.053
29. Paul NK, Jha M, Bhullar KS, et al. All trans 1-(3-arylacryloyl)-3, 5-bis(pyridin-4-ylmethylene)piperidin-4-ones as curcumin-inspired antineoplastics. *Eur J Med Chem*. 2014;87:461–470. doi:10.1016/j.ejmech.2014.09.090
30. Faria JV, Vegi PF, Miguita AGC, et al. Recently reported biological activities of pyrazole compounds. *Bio Org Med Chem*. 2017;25(21):5891–5903. doi:10.1016/j.bmc.2017.09.035
31. Khan MF, Alam MM, Verma G, et al. The therapeutic voyage of pyrazole and its analogs: a review. *Eur J Med Chem*. 2016;120:170–201. doi:10.1016/j.ejmech.2016.04.077
32. Min ZL, Hu XM. Tungstophosphoric acid-catalyzed synthesis of pyrazolones in water. *Asia J Chem*. 2013;25(13):7290–7292. doi:10.14233/ajchem.2013.14550
33. Chung AS, Lee J, Ferrara N. Targeting the tumor vasculature: insights from physiological angiogenesis. *Nat Rev Cancer*. 2010;10(7):505–514. doi:10.1038/nrc2868
34. Weber AM, Ryan AJ. ATM and ATR as therapeutic targets in cancer. *Pharmacol Ther*. 2015;149:124–138.